7. Abbreviations for the amino acid residues are as follows: A, Ala; C, Cys; D, Asp; E, Glu; F, Phe; G, Gly; H, His; I, Ile; K, Lys; L, Leu; M, Met; N, Asn; P, Pro; Q, Gln; R, Arg; S, Ser; T, Thr; V, Val; W, Trp; and Y, Tyr.
8. C. F. Scott, Jr., *et al.*, *Proc. Natl. Acad. Sci. U.S.A.* **87**, 8597 (1990); E. O. Freed, D. J. Myers, R. Risser, *J. Virol.* **65**, 190 (1991); E. Tschachler, H. Buchow, R. C. Gallo, M. S. Reitz, *ibid.* **64**, 2250 (1990).
9. E. A. Emini *et al.*, *J. Virol.* **64**, 3674 (1990).
10. M. Girard *et al.*, *Proc. Natl. Acad. Sci. U.S.A.* **88**, 542 (1991); P. W. Berman *et al.*, *Nature* **345**, 622 (1990).
11. Y. Devash, T. A. Calvelli, D. G. Wood, K. J. Reagan, A. Rubinstein, *Proc. Natl. Acad. Sci. U.S.A.* **87**, 3445 (1990).
12. P. Rossi *et al.*, *ibid.* **86**, 8055 (1989).
13. K. Javaherian *et al.*, *Science* **250**, 1590 (1990).
14. W. C. Koff and D. F. Hoth, *ibid.* **241**, 426 (1988); T. J. Matthews and D. P. Bolognesi, *Sci. Am.* **259**, 120 (October 1988).
15. J. P. Tam, *Proc. Natl. Acad. Sci. U.S.A.* **85**, 5409 (1988); D. N. Posnett, H. McGarth, J. P. Tam, *J. Biol. Chem.* **263**, 1719 (1988); J. P. Tam and Y.-A. Lu, *Proc. Natl. Acad. Sci. U.S.A.* **86**, 9084 (1989); J. P. Tam *et al.*, *J. Exp. Med.* **171**, 299 (1990).
16. Both monomeric and octameric peptide syntheses were accomplished by a stepwise solid-phase procedure with an automated peptide synthesizer on either a 4-methylbenzhydrylamine (MBHA) resin or an octamer resin that was prepared by three successive couplings of di-*tert*-butoxycarbonyl Lys onto the original MBHA resin (*15*). The protecting scheme for synthesis, which used a *tert*-butoxycarbonyl group for the α NH_2-terminus and side chain protecting groups for trifunctional amino acids, and the cleavage procedure were as described (*20*). Both the monomeric and octameric synthetic peptides were purified and analyzed by reversed-phase high-performance liquid chromatography (Millipore).
17. C. Y. Wang, M. Li, J. Ye, unpublished data.
18. D. J. Looney *et al.*, *Science* **241**, 357 (1988).
19. R. H. Meloen, R. M. Liskamp, J. Goudsmit, *J. Gen. Virol.* **70**, 1505 (1989).
20. J. J. G. Wang *et al.*, *Proc. Natl. Acad. Sci. U.S.A.* **83**, 6159 (1986).
21. Guinea pigs were bled by cardiac puncture with an appropriate restraining device. The animals were housed at Long Island Jewish Hospital, New Hyde Park, NY, with treatment and care under the approval of the institutional animal care and use committee of that institution.
22. B. Chesbro and K. Wehrly, *J. Virol.* **62**, 3779 (1988).
23. We thank L. Arthur for serum 505 (Frederick Cancer Research Center, Frederick, MD), H. Qiu and P. Badel for technical assistance, and F. Shen and J. Zheng for assistance in manuscript preparation. Supported in part by NIH grant IU01-AI-30238.

25 June 1991; accepted 11 September 1991

Modulation of the Time Course of Fast EPSCs and Glutamate Channel Kinetics by Aniracetam

CHA-MIN TANG,* QING-YAO SHI, ALEX KATCHMAN, GARY LYNCH

It is generally accepted that glutamate serves as the neurotransmitter at most excitatory synapses in the mammalian central nervous system (CNS). Synaptic release of glutamate may trigger a fast and a slow excitatory postsynaptic current (EPSC). The slow EPSC is mediated by *N*-methyl-D-aspartate (NMDA) receptor channels, whereas the fast EPSC is mediated by non-NMDA receptor channels. The nootropic agent aniracetam selectively and reversibly slows the desensitization kinetics of non-NMDA channels and lengthens their single-channel open times. Aniracetam also modulates the kinetics of the fast EPSC in a manner that mirrors its action on the kinetics of the non-NMDA channels. These results support the hypothesis that the properties of the non-NMDA glutamate channels rather than the rate of neurotransmitter clearance are the primary determinants of the kinetics of the fast EPSC in the mammalian CNS.

IN THE MAMMALIAN CNS, SYNAPTIC currents evoked by the synaptic release of glutamate can be separated into two distinct components, the fast EPSCs and the slow EPSCs, which are respectively mediated by the non-NMDA and the NMDA subtypes of the glutamate receptor channels (*1–4*). The mechanisms that determine the time course of these two EPSC components are important for understanding synaptically mediated phenomena in the mammalian CNS. Although the time course of the slow EPSC is determined by the long burst kinetics of the NMDA channels in response to a brief exposure to glutamate (*5*), the mechanism underlying the time course of the fast EPSC is not well understood. In the experiments described here a drug that acts selectively on the non-NMDA receptor channel, aniracetam, was used to test whether modulation of the kinetics of the non-NMDA channel alone would effect an equivalent change in the time course of the fast synaptic current.

Aniracetam belongs to a class of nootropic (cognitive-enhancing) agents whose mechanisms of action are poorly understood (*6*). Ito and co-workers, using the oocyte expression system, showed that aniracetam enhances currents mediated by non-NMDA receptors but not those associated with NMDA and γ-aminobutyric acid (GABA) receptors (*7*). The mechanism of this selective enhancement, however, remains unknown.

Under conditions that minimize the conductance through NMDA channels (*8*), step application of glutamate (500 μM) elicited a rapidly activating current that rapidly decayed despite the maintenance of a constant glutamate concentration. Figure 1A illustrates the ensemble-averaged currents recorded from an excised outside-out patch before and during application of aniracetam (1 mM). Aniracetam prolonged the rate of desensitization from 6.9 to 13.8 ms (trace marked *). In 17 other membrane patches aniracetam prolonged the rate of desensitization (±SD) from 5.5 ± 1.9 to 12.5 ± 5.5 ms. In a hippocampal slice, we evoked fast EPSCs in a CA1 neuron by stimulation of Schaffer commissural pathways (*9*) (Fig. 1B). In the presence of aniracetam (trace marked *) the rate of current decay changed from 6.5 to 10.9 ms (6.9 ± 0.5 to 11.4 ± 1.0 ms in four experiments). A secondary, less pronounced, and more variable effect of aniracetam was a modest increase in the initial current amplitudes. In both excised membrane patches and the brain slice the onset of aniracetam's actions was rapid (within tens of milliseconds in the case of excised patches) and easily reversible.

Miniature EPSCs (mEPSCs) are synaptic currents evoked by the spontaneous release

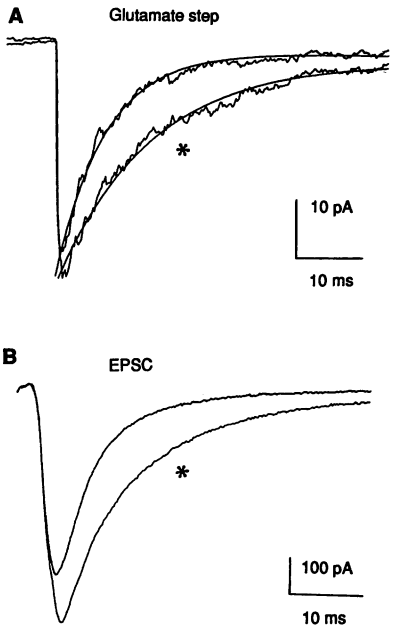

Fig. 1. Comparison of aniracetam's effects on non-NMDA glutamate channel desensitization kinetics (**A**) with its effects on the fast EPSC evoked in a CA1 neuron by stimulation of Schaffer commissural pathways in a rat hippocampal slice (**B**). In (A) the currents represent the ensemble average of recordings from ten consecutive step applications of glutamate (500 μM) on a single outside-out membrane patch. Holding potential, −80 mV in (A) and −70 mV in (B).

C.-M. Tang, Q.-Y. Shi, A. Katchman, Department of Neurology, University of Pennsylvania and the Graduate Hospital, Philadelphia, PA 19146.
G. Lynch, Bonney Center for Learning and Memory, University of California, Irvine, CA 92717.

*To whom correspondence should be addressed.

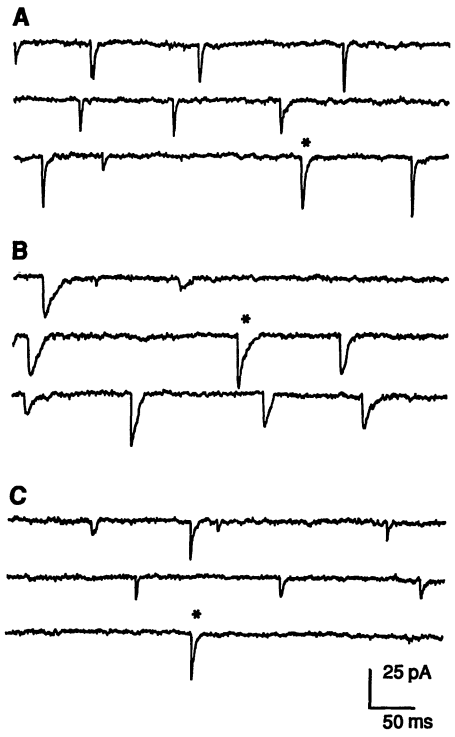

Fig. 2. Effects of aniracetam on fast spontaneous mEPSCs recorded from cultured hippocampal neurons. Aniracetam (1 mM) leads to a reversible prolongation of the fast mEPSCs. Time constants for representative individual mEPSCs (*) are (**A**) 3.3, (**B**) 7.9, and (**C**) 3.5 ms. Holding potential, −80 mV.

of discrete transmitter vesicles at individual synaptic boutons. mEPSCs provide an opportunity to examine the effects of aniracetam on the kinetics of synaptic currents independent of contributions from asynchronous transmitter release and other presynaptic factors. Fast mEPSCs can be prominently seen in hippocampal neurons that have been maintained in culture for longer than 10 days (*10*). NMDA- and GABA-mediated synaptic currents are minimized in the presence of external 1 mM Mg^{2+} and with the addition of 2-amino-5-phosphonovalerate (APV) (100 μM) and picrotoxin (100 μM). Recordings were restricted to neurons whose spontaneous mEPSCs exhibited rapid rise times (<1 ms) and a narrow distribution of decay time constants. Under these conditions, addition of antiracetam results in a significant prolongation of the time course of the fast EPSCs (Fig. 2). The averaged EPSC time constants (±SD, n = 70) before, during, and after application of aniracetam were, respectively, 3.1 ± 0.7, 8.0 ± 0.7, and 3.9 ± 1.8 ms (P < 0.001), and the peak amplitudes were 17 ± 8, 22 ± 6, and 17 ± 5 pA. The slight increase in EPSC amplitudes, rather than a decrease, and the absence of any resolvable changes in EPSC rise times eliminate the possibility that the prolongation of EPSC duration is due to the shift of activity of proximally located synapses to those located more distally. Further confirmation that these fast EPSCs are mediated by non-NMDA glutamate channels was shown by their complete elimination with addition of 1 μM 6-cyano-7-nitroquinoxalin-2,3-dione. These findings suggest that aniracetam modulates the fast EPSC at a postsynaptic site and that its action on the mEPSC mirrors its action on glutamate channel desensitization and electrically evoked fast EPSC.

To examine the molecular mechanisms underlying the action of aniracetam, we recorded single-channel events from four different patches using different experimental protocols (Fig. 3, A through D). Step applications of high concentrations of glutamate resulted in rapid channel activation followed by rapid closure (Fig. 3, A and B). The currents in Fig. 3A are carried predominantly by high-conductance (35 pS) channels (*11*) and in Fig. 3B by lower conductance channels (*12, 13*). Addition of aniracetam significantly prolonged channel openings without noticeable change in channel conductance. In order to better resolve the individual channel events, we applied lower concentrations of glutamate in 200-ms pulses as well as under steady-state perfusion (Fig. 3C). Histograms showing the distribution of individual open times were well fitted to single exponentials of 0.63 and 1.05 ms, before and during exposure to aniracetam (n = 229 and 372 openings). Figure 3, C and D, illustrates another

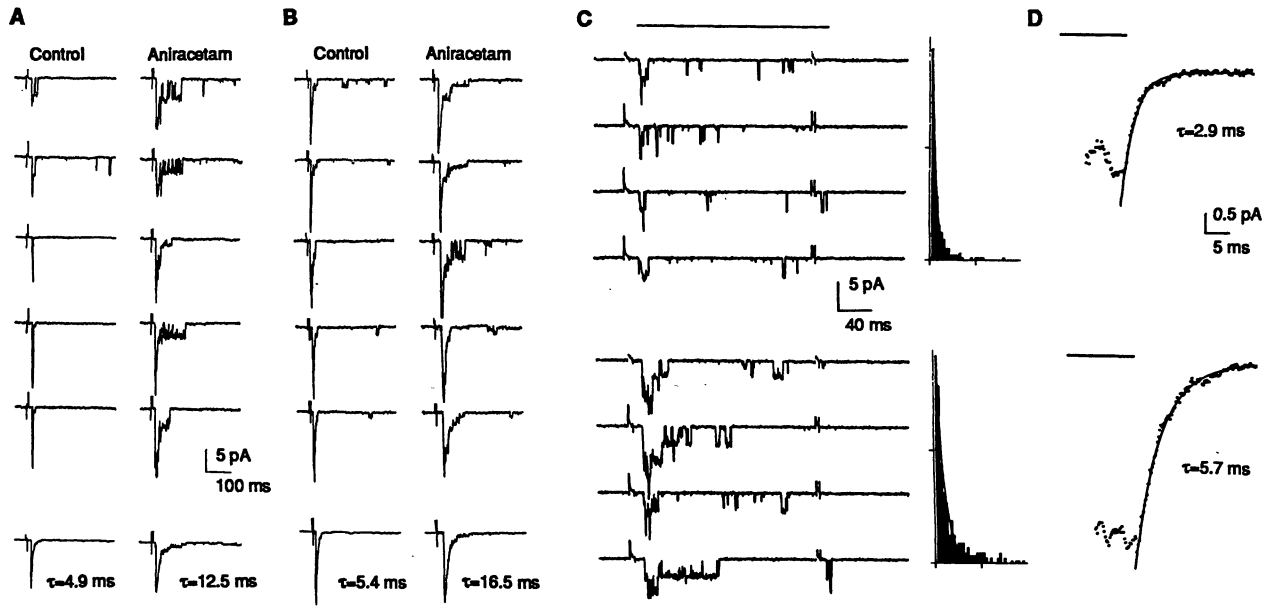

Fig. 3. Modulation of non-NMDA channel kinetics by aniracetam; changes at the single-channel level underlying aniracetam's modulatory action at the macroscopic level. Rapid step changes in glutamate concentration (0 to 1 mM) result in rapid but transient activation of high-conductance (35 pS) channels (in **A**) and lower conductance channels (in **B**). The bottom traces are the ensemble averages of ten individual traces. Aniracetam (1 mM) prolongs burst durations. Individual channel events become easier to resolve. In (**C**) we applied lower concentrations of glutamate (100 μM) to better resolve individual events. Upper traces were before and lower traces were during aniracetam application. Individual channel open times are shown in the histograms to the right (n = 229 before and 372 during aniracetam). In (**D**) the action of aniracetam on the kinetics of current termination as glutamate is rapidly stepped down is shown. The traces represent the ensemble average of ten individual traces from a patch containing many channels. Holding potential, −80 mV.

critical difference between NMDA and non-NMDA channels, their deactivation kinetics. Rapid removal of glutamate led to a rapid termination of non-NMDA–mediated currents. The ensemble average of currents during this rapid termination can be well fitted to a single exponential. Aniracetam prolonged the deactivation kinetics from 2.9 to 5.7 ms for the patch shown in Fig. 3D.

Desensitization at the macroscopic current level can be due to a number of different mechanisms operating at the microscopic single-channel level. Lectins such as concanavalin A (Con A) and wheat germ agglutinin (WGA) alter non-NMDA desensitization in an irreversible manner (*14, 15*). The lectins and aniracetam differ somewhat in their actions on synaptic currents. Con A does not alter EPSC kinetics (*14*). WGA prolongs the EPSC kinetics but primarily causes a significant increase in amplitudes of the EPSC (*15*). The reasons for these differences are not yet clear.

These data have several implications for the understanding of non-NMDA glutamate channels and synaptic phenomena subserved by them. First, these results and those reported earlier by Ito and co-workers (7) show that aniracetam can be used to selectively modulate fast excitatory synaptic currents. Aniracetam can also be effectively used to slow the kinetics of non-NMDA channel so that they can be better resolved. Second, these results have significant implications for hypotheses regarding the mechanisms responsible for the expression of long-term potentiation (LTP). The increase caused by aniracetam in the amplitude of synaptic responses is reduced by almost 50% after induction of LTP (*16*), and the time point in the response at which the drug begins to act is delayed (*17*). Manipulations that enhance release do not cause effects of these kinds (*16, 17*). In light of aniracetam's actions on channel kinetics, the most plausible explanation is that induction of LTP alters the properties of the postsynaptic receptors. Third, these data directly verify for the case of the glutamate-mediated EPSC a generalized form of a hypothesis initially proposed by Magleby and Stevens (*18*). This hypothesis postulates that the time course of EPSCs is determined by the kinetics of the postsynaptic receptors in response to a very brief exposure of the neurotransmitter. In the case of the fast EPSC, however, the validity for the assumption that the neurotransmitter lifetime within the synaptic cleft is much shorter than the duration of the EPSC is unclear (*11, 13*). These data show that, independent of the possible kinetics of neurotransmitter clearance, the time course of the fast EPSC in the mammalian CNS is predominantly determined by the kinetics of the non-NMDA receptor-channel complex.

REFERENCES AND NOTES

1. I. D. Forsythe and G. L. Westbrook, *J. Physiol. (London)* **396**, 515 (1988).
2. G. L. Westbrook and C. E. Jahr, *Sem. Neurosci.* **1**, 103 (1989).
3. C. F. Zorumski, J. Yang, G. D. Fischbach, *Cell. Mol. Neurobiol.* **9**, 95 (1989).
4. S. Hestrin, R. A. Nicoll, D. J. Perkel, P. Sah, *J. Physiol. (London)* **422**, 203 (1990).
5. R. A. J. Lester, J. D. Clements, G. L. Westbrook, C. E. Jahr, *Nature* **346**, 565 (1990).
6. W. Frostl and L. Maitre, *Pharmacopsychiatry* (Suppl.) **22**, 54 (1989).
7. I. Ito, S. Tanabe, A. Kohda, H. Sugiyama, *J. Physiol. (London)* **424**, 533 (1990).
8. External solution contained 1 mM Mg^{2+} and no added glycine. Membrane potential was held at −80 mV. In some experiments MK-801 (10 μM) and APV (500 μM) were added to show that the high-conductance channels were not NMDA channels. We studied fast desensitization kinetics with a fast perfusion system that changed solutions by switching the flow from the two sides of a theta tubing pulled to a gradually tapering opening of 200 μm. Membrane patches were excised to yield outside-out configurations. Synaptic currents were recorded with the whole-cell configuration of the patch clamp technique in both the cultured neurons and the hippocampal slices. Internal pipette solutions are as in (*11*). Single-channel data were acquired with an integrating patch clamp amplifier (Dagan), filtered at 2 kHz, sampled at 4 kHz, and analyzed with PClamp (Axon Instrument).
9. Experiments were performed with the "blind" whole-cell patch clamp technique in hippocampal slices. Slices from young adult rats were maintained in an interface chamber at 35° ± 1°C with the upper surface of the slices exposed to an atmosphere of humidified 95% O_2 and 5% CO_2. Conventional perfusion medium (flow rate, 1 ml/min) was used. Patch clamp pipettes had resistances of 4 to 7 megohms when filled with an intracellular solution composed of the following: 130 mM cesium gluconate, 10 mM KCl, 10 mM Hepes, 2 mM adenosine triphosphate, 0.2 mM guanosine triphosphate, pH = 7.3, 275 mosmol. On approach to a cell, gentle suction was applied to the pipette until a gigaseal was obtained (typically 1 to 10 gigaohms). A holding potential of −70 mV was then applied and the membrane patch ruptured by suction. Typical whole-cell input resistance was 100 to 300 megohms. Synaptic currents were evoked by stimulation of Schaffer commissural afferents with electrodes positioned in the stratum radiatum proximal to the cell body layer. Priming stimulation was used to suppress inhibitory synaptic currents during the responses [J. Larson and G. Lynch, *Science* **232**, 985 (1986)].
10. Neurons were isolated from 20-day-old rat embryos, incubated in Ca^{2+}-free buffer, triturated, and plated in 35-mm tissue dishes that had been coated with a thin layer of Matrigel (Collaborative Research). Cells were maintained in minimum essential medium supplemented with 10% fetal bovine serum and 5% horse serum. Cytosine arabinoside (10 μM) was added when the background glial cell layer became confluent at about 1 week after initial plating.
11. C.-M. Tang, M. Dichter, M. Morad, *Science* **243**, 1474 (1989).
12. P. Ascher and L. Nowak, *J. Physiol. (London)* **399**, 227 (1988).
13. L. O. Trussell and G. D. Fischbach, *Neuron* **3**, 209 (1989).
14. M. L. Mayer and L. Vyklicky, *Proc. Natl. Acad. Sci. U.S.A.* **86**, 1411 (1989).
15. C. F. Zorumski, L. L. Thio, G. D. Clark, D. B. Clifford, *Soc. Neurosci. Abstr.* **16**, 547 (1990).
16. P. Xiao, U. Staubli, M. Kessler, G. Lynch, *Hippocampus*, in press.
17. U. Staubli, J. Ambros-Ingerson, G. Lynch, *ibid.*, in press.
18. K. L. Magleby and C. F. Stevens, *J. Physiol. (London)* **223**, 173 (1972).

19. Supported by a Klingenstein Foundation Award and NIH grant NS28158 (to C.-M.T.) and Air Force Office of Scientific Research grant 890383 (to G.L.). We thank M. Rogawski for helpful suggestions. We thank D. Groul for suggestions that helped with the culturing of cell and G. Clark for the use of Matrigel.

27 June 1991; accepted 27 August 1991

Laser Ablation Studies of the Role of the *Drosophila* Oocyte Nucleus in Pattern Formation

DENISE J. MONTELL, HAIG KESHISHIAN, ALLAN C. SPRADLING

Somatic and germline cells interact during oogenesis to establish the pattern axes of the *Drosophila* eggshell and embryo. The role of the oocyte nucleus in pattern formation was tested with the use of laser ablation. Ablation in stage 6 to 9 egg chambers caused partial or complete ventralization of the eggshell, phenotypes similar to those of eggs produced by *gurken* or *torpedo* females. Accumulation of *vasa* protein at the posterior pole of treated oocytes was also disrupted. Thus the oocyte nucleus is required as late as stage 9 for dorsoventral patterning within the follicle cells and for polar plasm assembly in the oocyte.

THE INITIAL ANTERIOPOSTERIOR and dorsoventral axes and the terminal patterns of the segmented body plan in *Drosophila* are established during oogenesis (*1*). In the ovary, each developing egg chamber contains approximately 1000 somatically derived follicle cells surrounding the 16 germline-derived cells of the oocyte–nurse cell complex (*2*). Communication between the somatic and germline cells contributes to patterning the oocyte (*3*), and also to organizing the eggshell layers produced by the overlying follicle cells (*4*), although exactly where and when developmentally significant information is transferred within egg chambers remains unknown.

D. J. Montell, Carnegie Institution of Washington, Baltimore, MD 21210.
H. Keshishian, Biology Department, Yale University, New Haven, CT 06510.
A. C. Spradling, Howard Hughes Medical Institute and Carnegie Institution of Washington, Baltimore, MD 21210.